NIH Public Access
Author Manuscript
Free Radic Biol Med. Author manuscript; available in PMC 2015 March 01.

Published in final edited form as:
Free Radic Biol Med. 2014 March ; 68: 315–325. doi:10.1016/j.freeradbiomed.2013.12.018.

NOX1 causes ileocolitis in mice deficient in glutathione peroxidase-1 and -2

R. Steven Esworthy[1], **Byung-Wook Kim**[2], **Joni Chow**[1], **Binghui Shen**[1], **James H Doroshow**[3], and **Fong-Fong Chu**[1,4]

[1]Department of Radiation Biology, Beckman Research Institute of City of Hope, Duarte, CA 91010

[2]Irell & Manella Graduate School of Biological Sciences, Beckman Research Institute of City of Hope, Duarte, CA 91010

[3]National Cancer Institute, Bethesda, MD 20816

Abstract

We previously reported that mice deficient in two Se-dependent glutathione peroxidases, GPx1 and GPx2, have spontaneous ileocolitis. Disease severity depends on mouse genetic background. While C57BL/6J (B6) GPx1/2-DKO mice have moderate ileitis and mild colitis, 129S1Svlm/J (129) DKO mice have severe ileocolitis. Since GPxs are antioxidant enzymes, we hypothesized that elevated reactive oxygen species (ROS) trigger inflammation in these DKO mice. To test whether NADPH oxidase 1 (Nox1) contributes to colitis, we generated B6 triple-KO (TKO) mice to study their phenotype. Since the *Nox1* gene is X-linked, we analyzed the effect of NOX1 on male B6 TKO and female B6 DKO with the Nox1+/− (het-TKO) genotype. We found that the male TKO and female het-TKO mice are virtually disease-free when monitored from 8 through 50 days of age. Male TKO and female het-TKO mice have nearly no signs of disease (e.g. lethargy and perianal alopecia) that is often exhibited in the DKO mice; further, the slower growth rate of DKO mice is almost completely eliminated in maleTKO and female het-TKO mice. Male TKO and female het-TKO mice no longer have the shortened small intestine present in the DKO mice. Finally, the pathological characteristics of the DKO ileum, including the high number of crypt apoptosis (analyzed by apoptotic figures, TUNEL and cleaved caspase-3 immunohistochemical staining), and high numbers of Ki-67-positive crypt epithelium cells and elevated levels of monocytes expressing myeloperoxidase are all significantly decreased in male TKO mice. The attenuated ileal and colonic pathology is also evident in female het-DKO mice. Furthermore, the male DKO ileum has 8-fold higher TNF cytokine levels than TKO ileum. *Nox1* mRNA is highly elevated in both B6 and 129 DKO ileum compared to that in WT mouse ileum. Taken together, we propose that ileocolitis in the DKO mice is caused by NOX1, which is induced by TNF. The milder disease in female het-TKO intestine is likely due to random or imprinted X-chromosome inactivation, which produces mosaic *Nox1* expression.

© 2013 Elsevier Inc. All rights reserved.

[4]Correspondence: Fong-Fong Chu, Department of Radiation Biology, Beckman Research Institute of City of Hope, 1500 Duarte Road, Duarte, CA 91010-3000, fchu@coh.org, Tel: 626-256-HOPE x63831, Fax: 626-930-5330.

Publisher's Disclaimer: This is a PDF file of an unedited manuscript that has been accepted for publication. As a service to our customers we are providing this early version of the manuscript. The manuscript will undergo copyediting, typesetting, and review of the resulting proof before it is published in its final citable form. Please note that during the production process errors may be discovered which could affect the content, and all legal disclaimers that apply to the journal pertain.

NIH-PA Author Manuscript
NIH-PA Author Manuscript
NIH-PA Author Manuscript

NIH-PA Author Manuscript

NIH-PA Author Manuscript

NIH-PA Author Manuscript

Keywords

apoptosis; C57BL/6J; glutathione peroxidase; GPx1; GPx2; inflammatory bowel disease; NADPH oxidase; Nox1; mouse ileum and colon; TNF

Introduction

We have reported that mice deficient in two selenium-dependent glutathione peroxidases, GPx1 and GPx2-double knockout (DKO) mice, have spontaneous ileocolitis under conventional housing conditions [1][2]. Mouse genetic background has a huge impact on the severity of inflammation; while 129S1Svlm/J (129) DKO mice had severe colitis; C57BL6/J (B6) mice had very mild colitis but moderate ileitis [3]. Independent of genetic background, a characteristic pathology present in the gut epithelium of the GPx1/2-DKO mice is elevation of proliferating and apoptotic cells; the DKO mice have 2.2- and 2.8-fold higher numbers of bromodeoxyuridine (BrdU)-positive mitotic epithelial cells in the crypt base of the ileum and colon, respectively, than non-DKO control mice [2]. Both the GPx1/2-DKO and GPx2-KO mice also have highly elevated levels of apoptotic epithelial cells analyzed by TUNEL assay and morphology in the crypt base of ileum and colon [2, 4, 5]. Because GPx2 mRNA and protein is highly expressed in the crypt base [5–7], these results suggest that GPX2 protects the crypt epithelium from oxidant-induced proliferation and apoptosis. However, the major source of reactive oxygen species (ROS) is unknown.

NOX1, a member of the ROS-generating NADPH oxidase family, is highly expressed in the colon epithelium, and is expressed at a much lower level in normal small intestinal mucosa [8]. NOX1-produced ROS have been shown to promote cell proliferation by activation of Wnt/β-catenin and Notch1 signaling in mouse colon [9]. Nox1-KO colon epithelium has 30% fewer BrdU-positive mitotic cells resulting in a 50% decrease in colonocytes but a 2-fold increase in mucin-containing goblet cells compared to wild-type (WT) mice [9]. Wnt signaling activates NOX1 via Rac1 GTPase activation to generate ROS, which inactivates suppressors in the Wnt/β-catenin pathway to accelerate cell proliferation [9–11]. We questioned whether NOX1 contributes to the excessive mitosis in the GPx1/2-DKO mice in this study.

The *Nox1* gene is located on the X-chromosome (www.NCBI.nlm.nih.gov). *Nox1* gene expression is highly induced by TNF (16-fold) and moderately induced by IFN-γ (3-fold) in T84 colon cancer cells [12]. *Nox1* gene expression is also highly induced by lipopolysaccharide (LPS) in macrophages [13]. In addition to induction of gene expression, TNF also activates NOX1 enzyme activity by forming a complex with Rac1 [13]. A downstream effect of TNF activation of NOX1 is to induce cell death. One study showed that TNF binds to TNF receptor 1 (TNFR1) and riboflavin kinase (RFK) to activate NOX1 leading to cell death [14]. Another group showed that agonist binding to TNF-related apoptosis-inducing ligand (TRAIL) receptors, death receptors 4 (DR4) and 5 (DR5), activates RFK and NOX1 to induce apoptotic death in cancer cell lines [15]. However, whether NOX1 induces apoptosis in normal intestinal epithelial cells has not been demonstrated.

In this manuscript, we provided the first evidence to demonstrate that NOX1 plays a major role in producing ileocolitis in the GPx1/2-DKO mice. The ileocolitis detected in the DKO mice is completely abolished in male TKO mice and substantially diminished in female het-TKO mice. We found that *Nox1* mRNA levels are highly elevated in the B6 and 129 DKO ileum, reaching the same levels as the colon. Additionally, male B6 DKO ileum has 8-fold higher TNF levels than B6 TKO ileum. Taken together, our findings suggest that the

NIH-PA Author Manuscript

NIH-PA Author Manuscript

NIH-PA Author Manuscript

ileocolitis in the DKO mice is related to NOX1-induced ROS, which is activated by TNF in the ileum.

Materials and Methods

Mice- The C57BL6/J (B6) GPx1/2-DKO mouse colony was derived from a mixed line of B6 and 129 strains [1] and were backcrossed to B6 for 7 generations [16]. B6 Nox1-KO mice were kindly provided by Karl-Heinz Krause (Geneva University, Switzerland). We used a breeding scheme to generate GPx1/2-DKO and male GPx1/2-Nox1-TKO or female het-TKO mice as littermates and often as full or half-sibs. WT B6 colony was housed on the same rack as the DKO line. The 129 DKO mouse colony was established as described previously [3]. Except for the 129 DKO colony which is fed with semi-purified diets (Harland Teklad; TD 06306 and TD 06307), all mice were reared on LabDiet (Purina). Mice were weighed and inspected for disease signs (perianal alopecia and redness, wet tail, diarrhea as well as lethargy) daily from 8–12 days of age till euthanasia at 48–51days of age. All studies conducted were approved by the City of Hope Institutional Animal & Use Committee.

Parameters and sampling- At necropsy the length of small and large intestine (excluding cecum) was recorded. One cm sections of the ileum (adjacent to the cecum) and rectum were harvested and immersed in RNAlater (Qiagen). A section each of ileum and the mid-colon was frozen for cytokine analysis. An additional 4 to 8 cm of the ileum and the remaining colon and cecum were processed for histological analysis.

Histological analysis- Formalin-fixed tissue sections were stained with hematoxylin and eosin (H&E). Sections were scored for inflammation pathology based on a 14-point system as previously described [3]. Scores of 0–6 generally reflect presence of crypt apoptosis/hyperproliferation, Paneth cell and mucin depletion without signs of acute inflammation. For scores greater than 6, acute inflammation is generally evident showing neutrophil infiltration, crypt/gland abscesses or erosion of the epithelium [3, 17]. Apoptosis was analyzed by cell morphology, and by the TUNEL method to detect DNA strand breaks using ApopTag Peroxidase In Situ Apoptosis Detection Kit (Millipore), as well as cleaved caspase-3 antibody (Cell Signaling; #9664) staining in sections. Cell proliferation was analyzed with mitotic figures and immunohistochemistry (IHC) of anti-Ki-67 antibody (DAKO Cytomation; #M7249). Monocytes and neutrophils were detected by anti-myeloperoxidase (MPO) antibody (Thermo Scientific; #PA5-32512). Crypt density was scored from four 10X fields of the ileum section per mouse. All analyses were done in a blinded fashion.

Detection of TNF cytokine- A 1-cm section of the frozen ileum was sonicated in 0.5 ml of lysis buffer (Tissue Extraction Reagent I, BioSource Inc, Camarillo, CA) supplemented with protease inhibitor cocktail (P8340, SIGMA) and phenylmethane-sulfonyl fluoride (SIGMA). Tissue homogenate was centrifuged at 10,000 × g for 1 min. The supernatant was assayed for protein concentration using BSA as standard with BCA method (Thermo Scientific). Five μl of supernatant was assayed for TNF using AlphaLISA Tumor Necrosis Factor α (mouse) Research Kit (AL505C, PerkinElmer, Waltham, MA). AlphaLISA assay is based on fluorescence resonance energy transfer technology, the fluorescence was detected with a alphascreen filter (Excited at 680, emitted at 570) with PHERAstar plate reader (BMG Labtech, Durham, NC). All assays were done in duplicates, triplicates or quadruplicates.

Real-time quantitative PCR- For synthesis of cDNA, ileum tissues stored in RNAlater (Qiagen) were homogenized with a Polytron homogenizer (PT 1200E: Brinkmann Kinematica, Fisher Scientific) and sonicated. Total RNA was isolated using the RNeasy

NIH-PA Author Manuscript

NIH-PA Author Manuscript

NIH-PA Author Manuscript

Mini kit (Qiagen). cDNA was synthesized from 2 μg total RNA by using M-MLV reverse transcriptase (Promega, Madison, WI, USA) in the presence of random hexamers (1 μg; Invitrogen). Real-time quantitative PCR (qPCR) was performed with the Eva qPCR SuperMix kit containing SYBR green dye (BioChain Institute, Hayward, CA, USA) and using an iQ5 Detection system (Bio-Rad Laboratories, Hercules, CA, USA). Data analysis was done as previously reported [16]. RNA quantity was normalized to β-actin. Each assay was performed in duplicate. Primer sequences are listed in Table 1.

Statistical analysis- Comparison of different groups for most studies was done with 1-way ANOVA, Tukey's multiple comparison tests. The exceptions were that Ileum and distal colon pathology scores (Fig 3D and Fig 4D) were analyzed using Kruskal-Wallis test with Dunn's multiple comparison test. Also, the colon length between male DKO and TKO (Fig 2B) was analyzed with t-test. When $P<0.05$ is considered significant. All tests were done with GraphPad PRISM, version 6.01.

Results

Male GPx1/2-Nox1-TKO and female het-TKO mice have diminished signs of disease and growth retardation characteristic of GPx1/2-DKO mice

We monitored disease signs in B6 GPx1/2-DKO and male GPx1/2-Nox1-TKO as well as female het-TKO mice. B6 DKO mice have mild signs of disease [3]; most commonly lethargy, which lasted 2–3 days occurring at 28–33 days of age when there was no weight gain. Additional disease signs, such as dampness at the base of tail and persistent perianal alopecia or irritation (redness) commencing soon after weaning were detected in 4 of 27 female and 2 of 23 male DKO mice. One of 50 DKO mice in this study lapsed into morbidity, precipitating at 30 days, marked by perianal inflammation, sustained weight loss and lethargy. In contrast, male B6 TKO and female het-TKO mice appeared normal; the maximum disease sign was 1 day of dampness at the tail base in 4 of 29 animals.

Because DKO mice have growth retardation, and body weight is gender-dependent [1], we analyzed body weight separately in male and female mice. In male mice, the DKO mice had significantly lower (11.6%; $P=0.04$) body weight than non-DKO controls at 22 days of age presumably due to early onset colitis [1], while the TKO mice had normal weight gain similar to non-DKO mice with at least a WT *GPx1* or *GPx2* allele (Fig 1). By 31 days of age, the male DKO were 18% lighter than TKOs and non-DKO controls. The weight difference in female mice between DKO and non-DKO or het-TKO (Nox1+/−) was less (9%) severe by 31 days of age, but still significant. The cessation of weight gain at 30–31days of age was temporary and the mice recovered to gain weight at a normal rate. Thus, the weight difference between DKO and other groups was kept constant after 31 days of age.

Male GPx1/2-Nox1-TKO mice do not demonstrate foreshortened small and large intestines and have normal ileum crypt density compared to male GPx1/2-DKO mice

We have reported that 129 strain GPx1/2-DKO mice have shortened colons compared to 129 WT and non-DKO mice [16]. Here, we found that the small intestine of 48- to 51-day-old male B6 DKO mice was 29.9±1.6 cm in length compared to 36.7±2 cm in TKO mice, i.e. 19% shorter ($P< 0.01$)(Fig 2A). The small intestine of the male TKO mice had the same length as male non-DKO and WT mice regardless of *Nox1* genotype. The shortened DKO small intestine seems to result from intestinal growth cessation starting at 31 days of age, when the body weight gain halted (Fig 1A and 3A). The male DKO intestine at 31-day-old was 31±0.3 cm long, while at 35 days was 29.8±1.9 cm. In contrast, the male non-DKO control (Nox1− and Nox1+) small intestine at 31-day-old was 33.1±1.8 cm (6–7%

NIH-PA Author Manuscript

NIH-PA Author Manuscript

NIH-PA Author Manuscript

difference vs. DKO; P=0.045 vs. DKO), at 35 days was 35±1.2 cm and at 48–51 days was 36.7±1.5 cm. At both 35 and 48–51 days, the length of non-DKO small intestine is significantly longer than DKO mice (P≤0.003)(Fig 2A and 3A). Since the DKO mice have mild colitis, their colon was only slightly shortened. The only significant difference was found that male DKO colon was 7.6% shorter than male TKO colon (P= 0.02) (Fig 2B).

The length of the small intestine of female DKO mice (31.6 ± 3.6 cm) is also significantly shorter than that of non-DKO (36.1±1.9 cm; P<0.02) and het-TKO mice with *Nox1*$^{+/-}$ genotype (Fig 2C). The reason that female het-TKO mice have longer small intestine than DKO mice is likely due to random or imprinted X-chromosome inactivation to produce NOX1-null in half of intestinal epithelial cells [18]. Consistent with the mild colitis status, female DKO colon is not shorter than TKO or non-DKO mice (Fig 2D).

Since increases in intestinal length are largely contributed by crypt fission, which will increase crypt density [19], we assessed whether the ileum in DKO mice has lower crypt density. By counting the number of crypts in a 10X field (~2 mm), we found that both male and female DKO ileum had fewer crypt counts than WT mice analyzed at 48–51 days of age (Fig 3B). The male DKO mice had the lowest counts (26.4±2.9 crypts/10X field) comparing to TKO (40.9±1.8 crypts/10X field), WT Nox1− (41.5±4.4) and WT Nox+ (43.25±4.4; P≤0.26). Both female DKO and het-TKO ileum had lower crypt densities than WT mice. The lower crypt density in the DKO ileum could reflect the distorted and enlarged crypt morphology (see below).

Male TKO and female het-TKO ileum and colon no longer have robust apoptosis in the crypt epithelium characteristic of GPx1/2-DKO mice

A hallmark of DKO intestinal pathology is elevated levels of apoptosis and mitotic cells (BrdU-positive crypt cells) in the crypt epithelium studied in B6;129 mixed and 129 strain mice [2] (and our unpublished observation). B6 DKO mice also have a 4- to 5-fold higher number of apoptotic figures in the ileal and colonic crypts compared to WT mice at ~50 days of age based on morphological assessment (Fig 4A,C,E and Fig 5A,C,E). Both male and female TKO ileum and colon had the same low levels of apoptotic figures as the WT mice. The morphological analysis is based on nuclear condensation and fragmentation, which is a unique feature associated with apoptosis [20]. To substantiate the apoptotic nature of cell death in DKO intestine, we also applied TUNEL assays (Sup Fig 1 and 2) and cleaved caspase-3 IHC (Sup Fig 3) to mouse ileum and colon. TUNEL assay detects DNA fragmentation based on terminal deoxynucleotidyl transferase-mediated dUTP nick-labeling with high sensitivity, and DNA fragmentation is a hallmark of apoptosis [21]. Both male and female DKO ileum had significantly higher TUNEL-positive cells than TKO and WT mice. While female DKO colon also had significantly higher number of TUNEL-positive cells than mice of other genotypes, the higher number of TUNEL-positive cells in male DKO colon did not reach statistical significance. There is a high correlation (R^2=0.70) between the morphological and TUNEL assays (Sup Fig 1C).

Caspase-3 is an effector caspase, which is activated during apoptosis irrespective of the specific-death-initiating stimuli [22]. Consistent with two other apoptotic assays, the DKO ileum had significantly higher number of cells stained with cleaved caspase-3 than the TKO ileum analyzed on male mice (Sup Fig 3). The number of positively stained cells for cleaved caspase-3 was a fraction (63%) of theTUNEL-positive cells, suggesting that other effector caspases, such as caspase-6 and -7, may be involved in apoptosis in the DKO intestine [22, 23]. However, the number of cleaved-caspase 3 positive cells is also highly correlated (R^2=0.71) with the number of TUNEL-stained cells (Sup Fig 3C).

NIH-PA Author Manuscript

NIH-PA Author Manuscript

NIH-PA Author Manuscript

Because 129 GPx2-KO mice also had elevated apoptotic figures in the colon [24], we also analyzed B6 GPx2-KO ileum to determine whether it had elevated apoptotic figures using morphological analysis. While B6 GPx2-KO (GPx1+/−) ileum had significantly lower number of apoptotic figures than B6 DKO mice, deletion of Nox1 further decreased the apoptotic index (Sup Fig 4). The moderate elevation in apoptosis in the B6 GPx2-KO ileum did not result in gross pathology (scores of 1).

These results suggest that NOX1 is a major source of ROS that induces apoptosis in the ileum and colon crypt epithelium of B6 DKO and GPx2-KO mice.

Male TKO and female het-TKO ileum and colon crypts have lower numbers of Ki67-positive cells than the DKO mice

We reported previously that B6;129 and B6 DKO mice have high rates of proliferation in the ileum and colon detected with IHC staining of cells incorporating BrdU [2, 25]. However, when we analyzed mitotic figures on H&E stained tissues of 129 GPx1/2-DKO mice, the DKO colon did not have elevated mitotic cells [24]. Here, we first determined mitotic figures on H&E stained tissues, and did not find elevation of mitotic figures in the B6 DKO mouse ileum and colon (Fig 4F and 5F). We then used IHC to detect Ki-67, which is a nuclear non-histone protein highly expressed in proliferating cells and thus has been used as a marker for proliferating cells [26]. Similar to the BrdU study, there were nearly 100-times more cells expressed Ki-67 compared to cells having mitotic figures (in anaphase and telophase) in the crypts of the ileum and colon (Fig 6). Also, DKO ileum and colon had ~50% more Ki-67 positive cells than TKO or WT mice; i.e. male DKO ileum had 32.8±7.6 (mean±SD) vs. 21.7±3.5 KI-67 positive cells in male TKO and 21±3.9 in WT ileum (Fig. 6). Therefore, we conclude that DKO ileum and colon crypt has elevated number of cells expressing Ki-67 protein, a marker for cell proliferation.

Male TKO and female het-TKO ileum and colon demonstrate decreased evidence of inflammation-related tissue injury than GPx1/2-DKO mice

About 50% of B6 DKO mice have moderate ileitis, while none of TKO ileums were inflamed. B6 DKO ileum pathology is characterized by Paneth granule depletion, gland distortion, increased apoptotic cells and moderate levels of exfoliation (anoikis of epithelium based on observing cleaved-caspase-3 staining in nearly all exfoliated cells and absence of MPO staining)(Fig 4A). As previously noted, ileal pathology increased at post-weaning and rose quickly through 27–28 days of age, and then gradually until 51 days of age ([25] and data not shown). Here, we compared ileal pathology of ~50-day-old mice and found that male TKO mice had almost no pathological abnormalities (Fig 4D). While the female het-TKO ileum also had lower pathology scores than female DKO mice, due to the heterogeneity in the scoring, the difference was not statistically significant.

The mild colon pathology of B6 DKO mice is characterized by increased apoptosis, lack of goblet cells, and gland distortion (Fig 5A). The pathology was largely abolished in male TKO mice and was partially reduced (although not reaching statistical significance) in female het-TKO mice (Fig 5D). As noted before, the Nox1-KO colon has a characteristically high level of goblet cells (Fig 5C) [9].

Male B6 DKO ileum had more infiltrating inflammatory cells and higher TNF levels than TKO and WT mice

We noted before that B6 DKO ileum had ~9.6-fold higher number of monocytes in 8-month-old and ~2-fold higher in 1-month-old mice compared to age-matched non-DKO mice identified by MPO IHC [25]. To examine whether TKO ileum had fewer inflammatory cells, we performed MPO IHC on five 50-day-old DKO and six TKO mice. As expected,

NIH-PA Author Manuscript

NIH-PA Author Manuscript

NIH-PA Author Manuscript

MPO-positive cells were rarely found in crypt exfoliates of DKO mice indicating very little neutrophil infiltration (0, 1, 1, 3, and 3 MPO-positive exfoliates/ 1 cm ileum; ~500 crypts). Also, DKO ileum had a higher number of infiltrating monocytes (MPO-positive cells located in the submucosa) (Fig 7A). The number of monocytes in the DKO ileum ranged from 5–27 per 40X field (~0.5mm; mean=13.8±9) with median pathology score of 6 (range 5–8), whereas the TKO mice had 0.5±0.5 MPO+ cells per 40X field with pathology scores of 0–1 (Fig 7B). The number of monocytes in the 50-day-old TKO ileum is similar to the value obtained from two 28-day-old DKO mice (0.38 and 0.64 MPO+ cells per 40X field) with pathology scores of 3, although much lower than 2 other 28-day-old DKO mice (3.1 and 3.6 MPO+ cells/40× field) with pathology scores of 4. When we plotted the MPO+ cells against pathology scores, we found a positive correlation between the number of MPO+ cells and ileum pathology (R^2=0.71) (Fig 7C).

Since TNF is produced by monocytes and macrophages, and *Nox1* is highly inducible by TNF in colon cancer cells [12], we examined TNF protein levels in the ileum. The male DKO ileum had TNF levels of 17±12 pg/mg protein (mean ± SD), 8-fold higher than TKO ileum (2.0±1.0) (Fig 7D). The female DKO ileum appeared to have TNF levels (8.6±9.8) elevated over het-TKO ileum (2.2±2.1). However, because of the large variation in TNF levels in the female DKO mice, the difference in TNF levels between female DKO and het-TKO was not significant.

Nox1 mRNA is highly elevated in the ileum of DKO mice compared to WT mice

NOX1 mRNA is expressed at very low levels in normal human ileum but at high levels in normal human colon [8, 27]. However, the *Nox1* gene expression pattern may vary in different species; *Nox1* is highly induced by LPS from *H. pylori* in guinea pig gastric mucosa cells for example, but human stomach does not express Nox1 [27]. Thus, we analyzed mouse Nox1 mRNA levels to determine whether Nox1 is expressed in the ileum. We found that Nox1 mRNA is highly expressed in DKO, but not in WT, mouse ileum (Fig 8A). The elevated *Nox1* mRNA levels in both B6 and 129 DKO mouse ilea reach the same level as in the colon.

We also compared gene expression of other members of NADPH oxidase family, including *Nox2, Duox2* and *Nox4*, in the ileum (Fig 8B–D). Nox2 is mainly expressed in neutrophils and monocytes [28]. Unexpectedly, Nox2 mRNA levels were the same in the DKO and WT colon and ileum (Fig 8B). It is possible that most neutrophils were exfoliated and undergoing apoptosis and thus their mRNA could not be detected.

Duox2 expression is restricted to the epithelium in the intestine [29]. As we reported before in 129 strain ileum and colon, DKO mice had elevated Duox2 mRNA levels while WT mice had very low Duox2 mRNA levels (Fig 8C) [16]. Here, WT B6 ileum and colon had high baseline Duox2 mRNA levels; no further increase in Duox2 mRNA levels were detected in the B6 DKO mice.

Another member of the NADPH oxidase family expressed in the intestine is Nox4, which is expressed in intestinal epithelial cells as well as blood vessels [30, 31]. Although Nox4 mRNA was elevated in B6 DKO compared to B6 WT ileum, no difference in Nox4 gene expression was detected in the 129 DKO and WT ileum (Fig 8D).

These results support the hypothesis that Nox1 gene expression is induced in mouse ileum by inflammation in the DKO mice.

NIH-PA Author Manuscript

NIH-PA Author Manuscript

NIH-PA Author Manuscript

Discussion

In this paper, we report that NOX1 promotes ileitis and colitis in both male and female B6 GPx1/2-DKO mice. Because the *Nox1* gene is on the X-chromosome, and mouse growth is gender dependent, we analyzed male Nox1-KO and female Nox1+/− or het-Nox1 mice separately. We reported previously that B6;129 DKO mice had retarded growth compared to their non-DKO littermates [1]. Here, we show that male B6 DKO mice had slower weight gain as early as 22 days of age, and by 31 days of age were 18% lighter than non-DKO mice. The female DKO mice also had growth retardation that was evident at 31 days of age. However, male GPx1/2-Nox1-TKO and female het-TKO mice no longer demonstrate growth retardation. While B6 DKO mice have mild signs of disease, including lethargy, wet tail, and perianal alopecia, TKO mice appeared normal. The normal growth and lack of disease signs in the TKO males and het-TKO females were the initial indications that NOX1 contributes to gut inflammation in the DKO mice. The diminished gut inflammation in the female het-TKO mice is likely due to the random or imprinted X-chromosome inactivation, which produces ~50% of epithelial cells that are Nox1-null.

Because the inflamed intestine often is shortened, we measured the length of small and large intestine as another indicator for inflammation. The DKO mice of both genders had significantly shorter small intestine than non-DKO and WT small intestine, whereas male TKO and female het-TKO small intestine had normal length. The shortened intestine likely results from prominent crypt cell death and loss of stem cells, which is reflected by 35% lower crypt density. B6 DKO ileum and colon has elevated crypt apoptosis estimated by apoptotic figures, TUNEL and cleaved caspase-3 staining. A similarly high level of apoptosis (0.9–1.0 apoptotic figure/crypt) in DKO ileum and colon occurs at 28 and 50 days of age, much higher than 0.2 apoptotic figures/crypt at 21 and 23 days of age (our unpublished data). The observation that TKO ileum and colon crypts do not have elevated levels of apoptosis suggests that NOX1 induces apoptosis in the DKO mice. The low level of apoptotic cells in the 21- and 23-day-old mice raises the possibility that Nox1 gene expression is elevated after 23 days of age.

DKO mice also have elevated proliferation in the crypts of ileum and colon (detected by BrdU incorporation into DNA), apparently to support epithelial growth in the face of rampant apoptosis [2]. Since BrdU incorporation during active DNA synthesis occurs during DNA replication and DNA repair [32], and BrdU incorporation can activate DNA damage responses [33], counting BrdU-labeled cells may overestimate the number of mitotic cells, especially when cells are undergoing apoptosis. Here, we detected elevated expression of Ki-67, a marker for cell proliferation, in the DKO but not TKO ileum and colon. When counting mitotic figures to determine cell proliferation, DKO ileum and colon did not have more mitotic counts than WT and TKO mice. Since the mitotic figure counts are two orders of magnitude lower than the number obtained from IHC staining of BrdU and Ki-67, it is possible that counting mitotic figures is not sensitive enough to detect a 50% difference. Coant et al. reported that Nox1-KO colon has 30% fewer BrdU-labeled cells compared to WT colon [9]. Taken together, it suggests that NOX1 promotes both cell apoptosis and proliferation in the DKO intestine.

B6 DKO mice have moderate ileitis with scores of 6–7 and mild colitis with scores of 1–2. This mild and moderate pathology is abolished in the TKO mice. In B6 DKO mice, there are few infiltrating neutrophils and most exfoliated cells are MPO-negative. Compared to the severe ileitis in 129 DKO mice, which have ~10 abscess /300 crypts, the B6 DKO ileum has ~1 abscess/300 crypts that are generally very small. Thus, it would be interesting to examine whether Nox1-KO also ameliorates ileocolitis in the 129 DKO mice, which have severe disease.

NIH-PA Author Manuscript

NIH-PA Author Manuscript

NIH-PA Author Manuscript

The DKO intestinal pathology most likely stems from ROS-induced cell death in the crypt epithelium, where GPX2 is highly expressed [5]. Crypt epithelium in GPx2-KO mice also has elevated apoptosis supporting the epithelium-driven pathogenesis. On the other hand, the ubiquitously expressed GPX1 has anti-inflammatory activities in many cell types including endothelial cells [34], intestinal epithelium from Salmonella-induced colitis [24], and lung epithelium from influenza A infection and cigarette smoke [35] [36]. GPx1-null leukocytes adhere to endothelial cells in cardiac tissue better than WT cells [37]. Therefore, GPx1 in epithelial or inflammatory cells can attenuate inflammatory responses. Adoptive transfer of bone marrow cells from WT mice to DKO mice is likely to alleviate inflammation in the gut exhibiting a phenotype similar to the GPx2-KO mice.

Nox1 expression in the gut is thought to be restricted to the colon epithelium [8]. However, we detected a high level of Nox1 mRNA in the DKO ileum, while the WT ileum has very low Nox1 mRNA levels. Although Nox1 is also expressed in macrophages [13, 38], since B6 DKO mice have very few inflammatory cells compared to epithelial cells, it is unlikely that the elevated Nox1 gene expression is contributed by the inflammatory cells. We will verify the epithelial expression of NOX1 protein when a NOX1-specific antibody becomes available.

We suspect that the ileal epithelial cells have elevated *Nox1* gene expression by responding to TNF, since it was reported that TNF induced Nox1 mRNA levels ~16-fold in T84 colon cancer epithelial cells [12]. Here, we detected elevated TNF levels in the ileum of male DKO mice compared to male TKO mice. Although the elevated TNF in the female DKO ileum was not statistically significant compared to het-TKO and WT ileum, clearly some of the female DKO mice also had a high level of TNF. Conceivably, the elevated TNF in the ileum induces the *Nox1* gene expression.

NOX1 is an executioner of TNF-induced apoptosis. TNF is a prominent stimulator of ROS production by activating multiple NADPH oxidases in the Nox family, including Nox1–4 and Duox2 by activation of TNF receptor 1 (TNFR1) or CD95 [39]. TNF activation of NOX1 is mediated through activation of riboflavin kinase (RFK), which forms a bridge between TNFR1 death domain and p22phox subunit of NOX1 [14]. RFK also bridges TNF-related apoptosis-inducing ligand (TRAIL) receptors and NOX1 to induce ROS-mediated apoptosis [15]. Since the high level of apoptosis characteristic in the DKO ileum and colon crypt epithelium is abolished in male TKO and female het-TKO mice, we may have provided the first in vivo example to establish the pro-apoptotic activity of NOX1.

Anti-TNF drugs, such as anti-human TNF monoclonal Ab (infliximab, IFX), have been successful in IBD therapy to induce and maintain remission in both Crohn's disease and ulcerative colitis [40]. However, a major concern for anti-TNF drug treatment is increases susceptibility to infection [41]. Also, a significant proportion of patients develop loss of response due to production of antibody to the anti-TNF drugs [40]. Since NOX1 mediates TNF-induced apoptosis and inflammation in the gut, it is possible that NOX1 inhibitors may also have efficacy for IBD therapy.

Thus, in this report, we have identified NOX1 to be a major contributor to intestinal epithelium apoptosis, proliferation, and ileocolitis in B6 GPx1/2-DKO mice. The pro-apoptotic activity and pro-inflammatory activity of NOX1 is likely induced by TNF, which is elevated in DKO ileum but not TKO ileum. Since anti-TNF drugs have been effective for IBD therapy but with significant drawbacks, conceivably, TNF effecters, such as NOX1 could be a drug target for IBD therapy.

NIH-PA Author Manuscript
NIH-PA Author Manuscript
NIH-PA Author Manuscript

Supplementary Material

Refer to Web version on PubMed Central for supplementary material.

Acknowledgments

We thank Sofia Loera and Tina Montgomery at Anatomic Pathology Core of City of Hope for tissue processing, and David Lu at High-Throughput Core for operating BMG PHERAstar plate reader. Research reported in this publication was supported by the National Cancer Institute of the National Institutes of Health under grant number P30CA033572. The content is solely the responsibility of the authors and does not necessarily represent the official views of the National Institutes of Health.

Abbreviations

BrdU	bromodeoxyuridine
GPx	glutathione peroxidase
GPx1/2-DKO	GPx1/2-double knockout
het-TKO	heterozygous-TKO or female GPx1/2-DKO Nox+/−
IBD	inflammatory bowel disease
MPO	myeloperoxidase
Nox1	NADPH Oxidase-1
TKO	GPx1/2-Nox1-triple knockout

References

1. Esworthy RS, Aranda R, Martin MG, Doroshow JH, Binder SW, Chu FF. Mice with combined disruption of Gpx1 and Gpx2 genes have colitis. Am J Physiol Gastrointest Liver Physiol. 2001; 281:G848–G855. [PubMed: 11518697]
2. Chu FF, Esworthy RS, Chu PG, Longmate JA, Huycke MM, Wilczynski S, Doroshow JH. Bacteria-induced intestinal cancer in mice with disrupted Gpx1 and Gpx2 genes. Cancer Res. 2004; 64:962–968. [PubMed: 14871826]
3. Esworthy RS, Kim BW, Larson GP, Yip ML, Smith DD, Li M, Chu FF. Colitis locus on chromosome 2 impacting the severity of early-onset disease in mice deficient in GPX1 and GPX2. Inflamm Bowel Dis. 2011; 17:1373–1386. [PubMed: 20872835]
4. Esworthy RS, Yang L, Frankel PH, Chu FF. Epithelium-specific glutathione peroxidase, Gpx2, is involved in the prevention of intestinal inflammation in selenium-deficient mice. J Nutr. 2005; 135:740–745. [PubMed: 15795427]
5. Florian S, Krehl S, Loewinger M, Kipp A, Banning A, Esworthy S, Chu FF, Brigelius-Flohe R. Loss of GPx2 increases apoptosis, mitosis, and GPx1 expression in the intestine of mice. Free Radic Biol Med. 2010; 49:1694–1702. [PubMed: 20828612]
6. Esworthy RS, Swiderek KM, Ho YS, Chu FF. Selenium-dependent glutathione peroxidase-GI is a major glutathione peroxidase activity in the mucosal epithelium of rodent intestine. Biochim Biophys Acta. 1998; 1381:213–226. [PubMed: 9685647]
7. Chu FF, Esworthy RS, Lee L, Wilczynski S. Retinoic Acid Induces Gpx2 Gene Expression in MCF-7 Human Breast Cancer Cells. J Nutr. 1999; 129:1846–1854. [PubMed: 10498757]
8. Szanto I, Rubbia-Brandt L, Kiss P, Steger K, Banfi B, Kovari E, Herrmann F, Hadengue A, Krause KH. Expression of NOX1, a superoxidegenerating NADPH oxidase, in colon cancer and inflammatory bowel disease. J Pathol. 2005; 207:164–176. [PubMed: 16086438]
9. Coant N, Ben Mkaddem S, Pedruzzi E, Guichard C, Treton X, Ducroc R, Freund JN, Cazals-Hatem D, Bouhnik Y, Woerther PL, Skurnik D, Grodet A, Fay M, Biard D, Lesuffleur T, Deffert C, Moreau R, Groyer A, Krause KH, Daniel F, Ogier-Denis E. NADPH oxidase 1 modulates WNT and

NIH-PA Author Manuscript

NIH-PA Author Manuscript

NIH-PA Author Manuscript

NOTCH1 signaling to control the fate of proliferative progenitor cells in the colon. Mol Cell Biol. 2010; 30:2636–2650. [PubMed: 20351171]

10. Leoni G, Alam A, Neumann PA, Lambeth JD, Cheng G, McCoy J, Hilgarth RS, Kundu K, Murthy N, Kusters D, Reutelingsperger C, Perretti M, Parkos CA, Neish AS, Nusrat A. Annexin A1, formyl peptide receptor, and NOX1 orchestrate epithelial repair. J Clin Invest. 2013; 123:443–454. [PubMed: 23241962]
11. Kajla S, Mondol AS, Nagasawa A, Zhang Y, Kato M, Matsuno K, Yabe- Nishimura C, Kamata T. A crucial role for Nox 1 in redox-dependent regulation of Wntbeta- catenin signaling. FASEB J. 2012; 26:2049–2059. [PubMed: 22278940]
12. Kamizato M, Nishida K, Masuda K, Takeo K, Yamamoto Y, Kawai T, Teshima-Kondo S, Tanahashi T, Rokutan K. Interleukin 10 inhibits interferon gamma- and tumor necrosis factor alpha-stimulated activation of NADPH oxidase 1 in human colonic epithelial cells and the mouse colon. J Gastroenterol. 2009; 44:1172–1184. [PubMed: 19714290]
13. Maitra U, Singh N, Gan L, Ringwood L, Li L. IRAK-1 contributes to lipopolysaccharide-induced reactive oxygen species generation in macrophages by inducing NOX-1 transcription and Rac1 activation and suppressing the expression of antioxidative enzymes. J. Biol. Chem. 2009; 284:35403–35411. [PubMed: 19850916]
14. Yazdanpanah B, Wiegmann K, Tchikov V, Krut O, Pongratz C, Schramm M, Kleinridders A, Wunderlich T, Kashkar H, Utermohlen O, Bruning JC, Schutze S, Kronke M. Riboflavin kinase couples TNF receptor 1 to NADPH oxidase. Nature. 2009; 460:1159–1163. [PubMed: 19641494]
15. Park KJ, Lee CH, Kim A, Jeong KJ, Kim CH, Kim YS. Death receptors 4 and 5 activate Nox1 NADPH oxidase through riboflavin kinase to induce reactive oxygen species-mediated apoptotic cell death. J. Biol. Chem. 2012; 287:3313–3325. [PubMed: 22158615]
16. Esworthy RS, Kim BW, Rivas GE, Leto TL, Doroshow JH, Chu FF. Analysis of candidate colitis genes in the gdac1 locus of mice deficient in glutathione peroxidase-1 and -2. PloS one. 2012; 7:e44262. [PubMed: 22970191]
17. Esworthy RS, Smith DD, Chu FF. A Strong Impact of Genetic Background on Gut Microflora in Mice. Int J Inflam. 2010; 2010:986046. [PubMed: 20976020]
18. Barakat TS, Gribnau J. X chromosome inactivation in the cycle of life. Development. 2012; 139:2085–2089. [PubMed: 22619385]
19. Dehmer JJ, Garrison AP, Speck KE, Dekaney CM, Van Landeghem L, Sun X, Henning SJ, Helmrath MA. Expansion of intestinal epithelial stem cells during murine development. PloS one. 2011; 6:e27070. [PubMed: 22102874]
20. Taylor RC, Cullen SP, Martin SJ. Apoptosis: controlled demolition at the cellular level. Nature reviews. 2008; 9:231–241.
21. Galluzzi L, Aaronson SA, Abrams J, Alnemri ES, Andrews DW, Baehrecke EH, Bazan NG, Blagosklonny MV, Blomgren K, Borner C, Bredesen DE, Brenner C, Castedo M, Cidlowski JA, Ciechanover A, Cohen GM, De Laurenzi V, De Maria R, Deshmukh M, Dynlacht BD, El-Deiry WS, Flavell RA, Fulda S, Garrido C, Golstein P, Gougeon ML, Green DR, Gronemeyer H, Hajnoczky G, Hardwick JM, Hengartner MO, Ichijo H, Jaattela M, Kepp O, Kimchi A, Klionsky DJ, Knight RA, Kornbluth S, Kumar S, Levine B, Lipton SA, Lugli E, Madeo F, Malomi W, Marine JC, Martin SJ, Medema JP, Mehlen P, Melino G, Moll UM, Morselli E, Nagata S, Nicholson DW, Nicotera P, Nunez G, Oren M, Penninger J, Pervaiz S, Peter ME, Piacentini M, Prehn JH, Puthalakath H, Rabinovich GA, Rizzuto R, Rodrigues CM, Rubinsztein DC, Rudel T, Scorrano L, Simon HU, Steller H, Tschopp J, Tsujimoto Y, Vandenabeele P, Vitale I, Vousden KH, Youle RJ, Yuan J, Zhivotovsky B, Kroemer G. Guidelines for the use and interpretation of assays for monitoring cell death in higher eukaryotes. Cell Death Differ. 2009; 16:1093–1107. [PubMed: 19373242]
22. Walsh JG, Cullen SP, Sheridan C, Luthi AU, Gerner C, Martin SJ. Executioner caspase-3 and caspase-7 are functionally distinct proteases. Proc Natl Acad Sci U S A. 2008; 105:12815–12819. [PubMed: 18723680]
23. Galluzzi L, Vitale I, Abrams JM, Alnemri ES, Baehrecke EH, Blagosklonny MV, Dawson TM, Dawson VL, El-Deiry WS, Fulda S, Gottlieb E, Green DR, Hengartner MO, Kepp O, Knight RA, Kumar S, Lipton SA, Lu X, Madeo F, Malorni W, Mehlen P, Nunez G, Peter ME, Piacentini M, Rubinsztein DC, Shi Y, Simon HU, Vandenabeele P, White E, Yuan J, Zhivotovsky B, Melino G,

NIH-PA Author Manuscript

NIH-PA Author Manuscript

NIH-PA Author Manuscript

Kroemer G. Molecular definitions of cell death subroutines: recommendations of the Nomenclature Committee on Cell Death 2012. Cell Death Differ. 2012; 19:107–120. [PubMed: 21760595]

24. Esworthy RS, Kim BW, Wang Y, Gao Q, Doroshow JH, Leto TL, Chu FF. The Gdac1 locus modifies spontaneous and Salmonella-induced colitis in mice deficient in either Gpx2 or Gpx1 genes. Free Radical Biology & Medicine. 2013 In Press.
25. Lee DH, Esworthy RS, Chu C, Pfeifer GP, Chu FF. Mutation accumulation in the intestine and colon of mice deficient in two intracellular glutathione peroxidases. Cancer Res. 2006; 66:9845–9851. [PubMed: 17047045]
26. Urruticoechea A, Smith IE, Dowsett M. Proliferation marker Ki-67 in early breast cancer. J Clin Oncol. 2005; 23:7212–7220. [PubMed: 16192605]
27. Rokutan K, Kawahara T, Kuwano Y, Tominaga K, Sekiyama A, Teshima- Kondo S. NADPH oxidases in the gastrointestinal tract: a potential role of Nox1 in innate immune response and carcinogenesis. Antioxid Redox Signal. 2006; 8:1573–1582. [PubMed: 16987012]
28. Rada B, Leto TL. Oxidative innate immune defenses by Nox/Duox family NADPH oxidases. Contrib Microbiol. 2008; 15:164–187. [PubMed: 18511861]
29. Geiszt M, Witta J, Baffi J, Lekstrom K, Leto TL. Dual oxidases represent novel hydrogen peroxide sources supporting mucosal surface host defense. FASEB J. 2003; 17:1502–1504. [PubMed: 12824283]
30. Schramm A, Matusik P, Osmenda G, Guzik TJ. Targeting NADPH oxidases in vascular pharmacology. Vascular pharmacology. 2012; 56:216–231. [PubMed: 22405985]
31. Barcellos-de-Souza P, Moraes JA, de-Freitas-Junior JC, Morgado-Diaz JA, Barja-Fidalgo C, Arruda MA. Heme modulates intestinal epithelial cell activation: involvement of NADPHox-derived ROS signaling. Am J Physiol Cell Physiol. 2013; 304:C170–C179. [PubMed: 23114967]
32. Kao GD, McKenna WG, Yen TJ. Detection of repair activity during the DNA damage-induced G2 delay in human cancer cells. Oncogene. 2001; 20:3486–3496. [PubMed: 11429695]
33. Masterson JC, O'Dea S. 5-Bromo-2-deoxyuridine activates DNA damage signalling responses and induces a senescence-like phenotype in p16-null lung cancer cells. Anti-cancer drugs. 2007; 18:1053–1068. [PubMed: 17704656]
34. Lubos E, Kelly NJ, Oldebeken SR, Leopold JA, Zhang YY, Loscalzo J, Handy DE. Glutathione Peroxidase-1 (GPx-1) deficiency augments proinflammatory cytokine-induced redox signaling and human endothelial cell activation. J. Biol. Chem. 2011
35. Yatmaz S, Seow HJ, Gualano RC, Wong ZX, Stambas J, Selemidis S, Crack PJ, Bozinovski S, Anderson GP, Vlahos R. Glutathione peroxidase-1 reduces influenza A virus-induced lung inflammation. Am J Respir Cell Mol Biol. 2013; 48:17–26. [PubMed: 23002098]
36. Duong C, Seow HJ, Bozinovski S, Crack PJ, Anderson GP, Vlahos R. Glutathione peroxidase-1 protects against cigarette smoke-induced lung inflammation in mice. Am J Physiol Lung Cell Mol Physiol. 2010; 299:L425–L433. [PubMed: 20511341]
37. Oelze M, Kroller-Schon S, Steven S, Lubos E, Doppler C, Hausding M, Tobias S, Brochhausen C, Li H, Torzewski M, Wenzel P, Bachschmid M, Lackner KJ, Schulz E, Munzel T, Daiber A. Glutathione Peroxidase-1 Deficiency Potentiates Dysregulatory Modifications of Endothelial Nitric Oxide Synthase and Vascular Dysfunction in Aging. Hypertension. 2013
38. Yeligar SM, Harris FL, Hart CM, Brown LA. Ethanol induces oxidative stress in alveolar macrophages via upregulation of NADPH oxidases. J Immunol. 2012; 188:3648–3657. [PubMed: 22412195]
39. Morgan MJ, Liu ZG. Reactive oxygen species in TNFalpha-induced signaling and cell death. Mol Cells. 2010; 30:1–12. [PubMed: 20652490]
40. Nanda KS, Cheifetz AS, Moss AC. Impact of antibodies to infliximab on clinical outcomes and serum infliximab levels in patients with inflammatory bowel disease (IBD): a meta-analysis. Am J Gastroenterol. 2013; 108:40–47. quiz 48. [PubMed: 23147525]
41. Blonski W, Lichtenstein GR. Safety of biologics in inflammatory bowel disease. Current treatment options in gastroenterology. 2006; 9:221–233. [PubMed: 16901386]

NIH-PA Author Manuscript

NIH-PA Author Manuscript

NIH-PA Author Manuscript

42. Goretsky T, Dirisina R, Sinh P, Mittal N, Managlia E, Williams DB, Posca D, Ryu H, Katzman RB, Barrett TA. p53 mediates TNF-induced epithelial cell apoptosis in IBD. Am J Pathol. 2012; 181:1306–1315. [PubMed: 22863952]

NIH-PA Author Manuscript

NIH-PA Author Manuscript

NIH-PA Author Manuscript

Highlights

- GPx1/2-DKO mice have spontaneous ileocolitis.
- DKO ileum has elevated TNF and Nox1 gene expression compared to wild type mice.
- Deletion of Nox1 in the GPx1/2-DKO mice ameliorates GI pathology.
- NOX1 is the major source of reactive oxygen species to cause ileocolitis in the DKO mice.

NIH-PA Author Manuscript
NIH-PA Author Manuscript
NIH-PA Author Manuscript

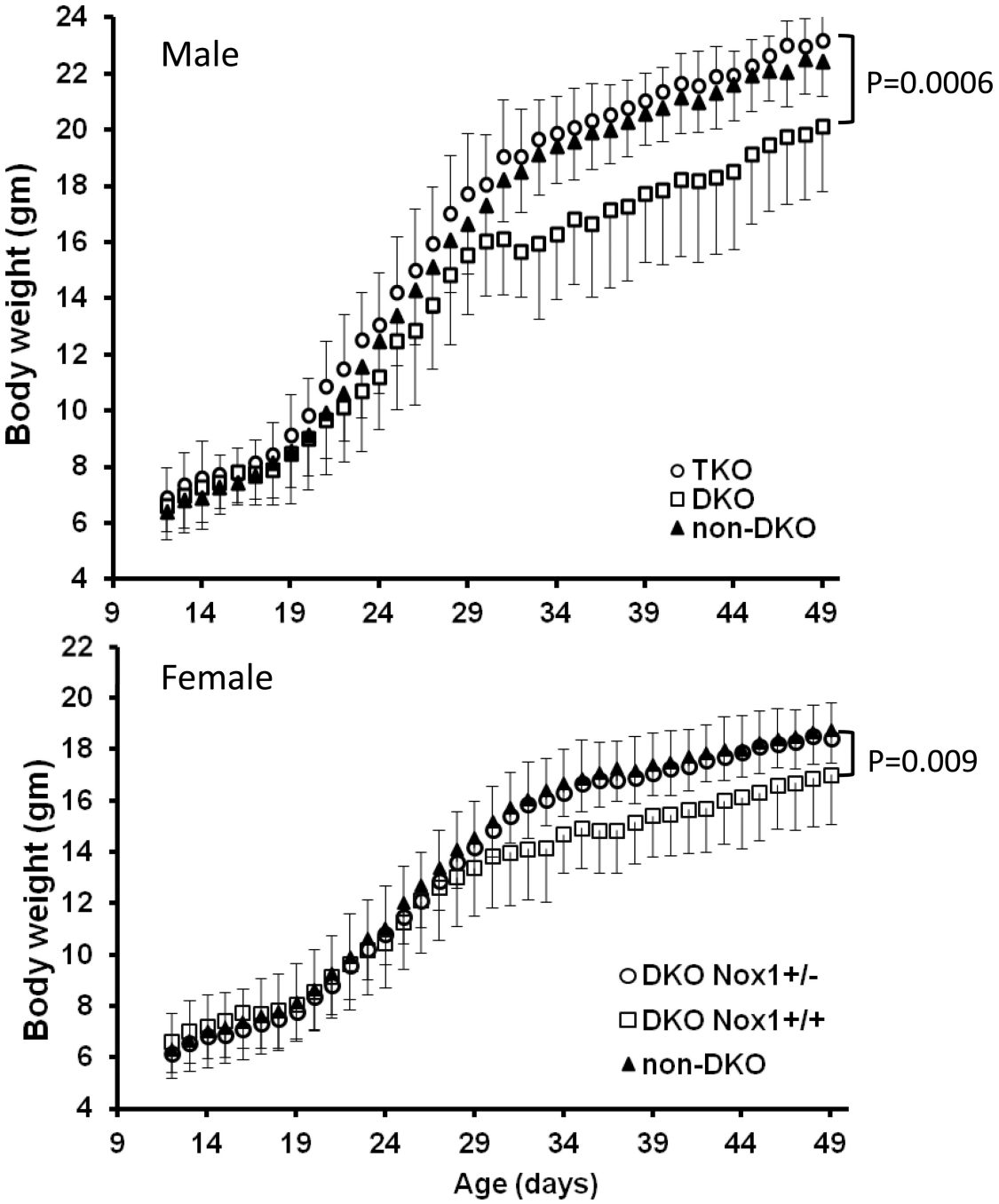

Figure 1.

Body weight of B6 GPx1/2-DKO (DKO), GPx1/2-Nox1-TKO (TKO) and non-DKO mice from 10 to 50 days of age. Panel A. Body weight of male B6 littermates from 23 DKO, 18 TKO and 12 non-DKO mice having one WT GPx1 or GPx2 allele with either Nox1 genotype. DKO males are significantly lighter than TKOs starting at 22 days of age (12%; P=0.008) with temporary halt in growth at days 31–33. From 31 days on, DKO mice weighed 17–18% lower than TKO and non-DKO mice (P≤ 0.0006). Panel B. Body weight of female B6 littermates from 27 DKO, 25 het-TKO and 15 non-DKO mice. Female DKOs weighed the same as TKOs through 29 days of age, then significantly lighter through 50

days of age. At day 30, P=0.046; P<0.009, thereafter). The error bars are 1 standard deviation (SD).

NIH-PA Author Manuscript
NIH-PA Author Manuscript
NIH-PA Author Manuscript

NIH-PA Author Manuscript
NIH-PA Author Manuscript
NIH-PA Author Manuscript

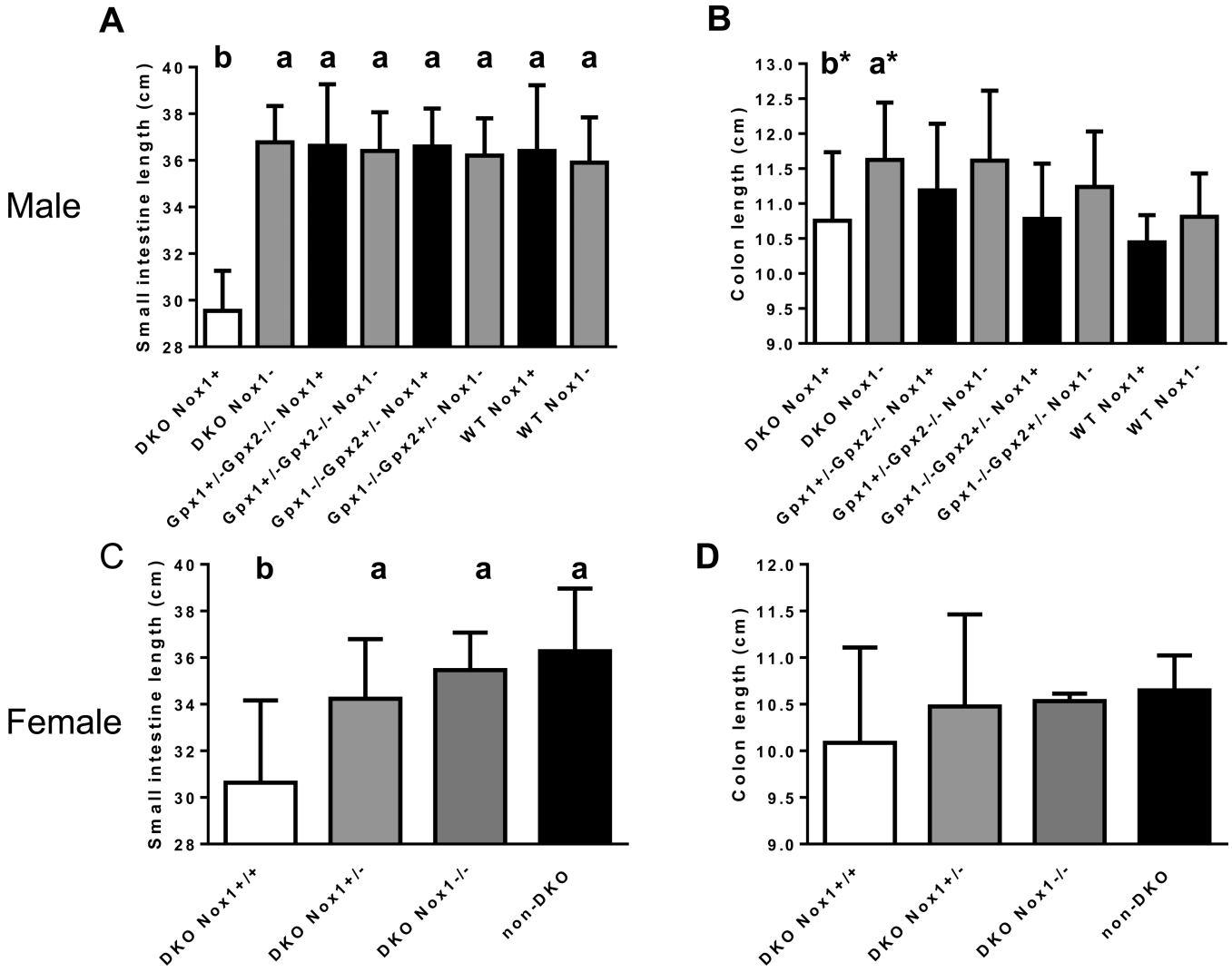

Figure 2.

The effect of *GPx1*, *GPx2* and *Nox1* gene on the length of small and large intestine in 50-day-old mice. Panel A. The length of small intestine in male mice. The number of mice in each group is 9 DKO, 9 TKO, 8 GPx1+/−GPx2−/−Nox1+, 11 GPx1+/− GPx2−/−Nox1−, 5 GPx1−/−GPx2+/−Nox1+, 3 GPx1−/−GPx2+/−Nox1−, 2 WT Nox+ and 2 WT Nox-. Panel B. The length of colon in male mice. The number of mice in each group is 22 DKO, 12 TKO, 9 GPx1+/−GPx2−/−Nox1+, 21 GPx1+/−GPx2−/−Nox1−, 6 GPx1−/− GPx2+/ −Nox1+, 5 GPx1−/−GPx2+/−Nox1−, 12 WT Nox+ and 26 WT Nox-. The group marked with a* and b* are different (a*>b*, t-test). However, there is no difference when analyzed with a multiple comparison test. Panel C. The length of small intestine in female mice. The number of mice in each group is 13 DKO, 22 het-DKO, 6 TKO and 5 non-DKO. Panel D. The length of colon in female mice. The number of mice in each group is 20 DKO, 25 het-DKO, 6 TKO and 6 non-DKO. The group with significant different length is marked with a different letter, where a>b. The error bars show one SD.

NIH-PA Author Manuscript

NIH-PA Author Manuscript

NIH-PA Author Manuscript

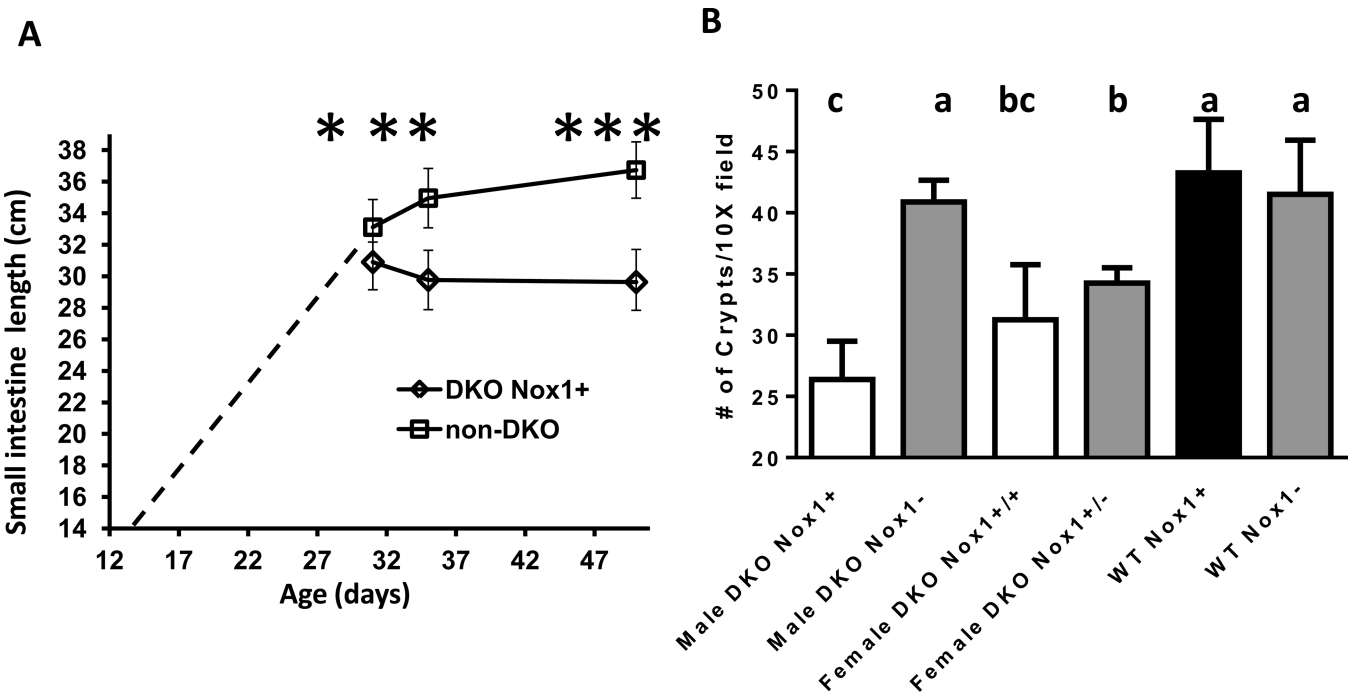

Figure 3.

Comparison of male small intestine length between 31, 35 and 50 days old and ileum crypt counts in 50-day-old mice of different genotypes. Panel A. The length of small intestine measured from DKO and non-DKO mice was from 31-, 35- and 50-day-old males. The dashed line from 14 days to 30 days is extracted from non-DKO mice (N=7, 4, 24, 12, 7 for 14, 19, 21, 28, 30 days of age, respectively). The number of mice in each group is: 9 DKO and 14 non-DKO each for 31-and 35-day-old, and 13 DKO and 29 non-DKO for 50-day-old. Error bars are SD. The asterisk signs indicate significant difference between the age-matched DKO and non-DKO groups as well as between non-DKO mice of 3 different ages. Variation in DKO ileal length across age is not significantly different. Panel B. Ileum crypt density determined from 4 areas (10X field or 2 mm each) of H&E stained tissue per mouse. The number of mice in each group is: 5 male DKO Nox1+, 6 male DKO Nox1−, 4 female DKO Nox1+/+, 4 female DKO NOx1+/−, 4 male WT Nox1+ and 6 male WT Nox1−. The counts from H&E stained tissue agreed with an independent assessment on Ki-67 IHC stained sections. The groups with different number of crypts have different letter, where a>b>c. The groups share the same letter are not different; i.e. bc is not different from b or c.

NIH-PA Author Manuscript
NIH-PA Author Manuscript
NIH-PA Author Manuscript

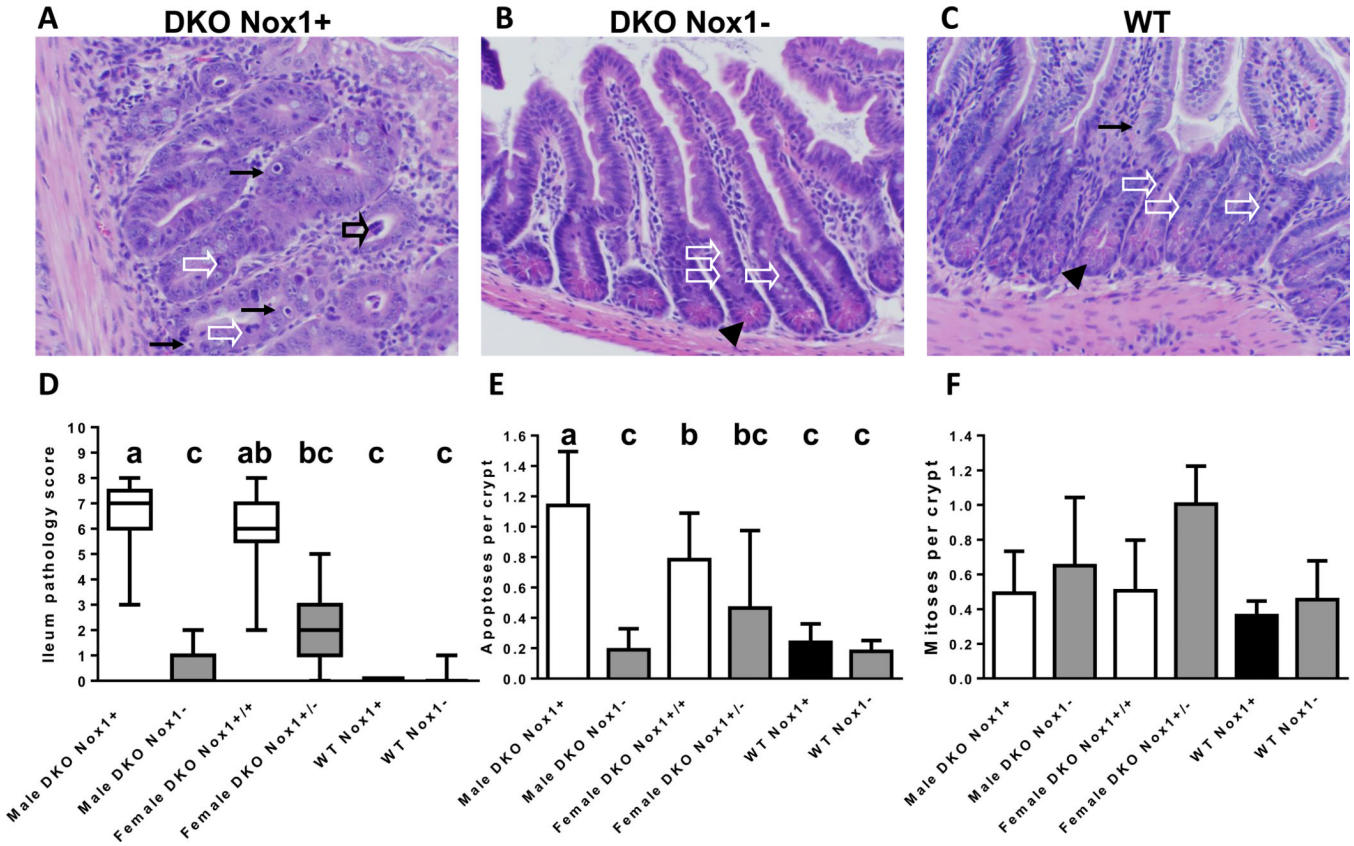

Figure 4.

Ileal histology, pathology scores and number of apoptotic and mitotic figures per crypt determined in 50-day-old mice. Panel A-C are H&E-stained ileal sections from a representative male DKO (A), TKO (B) and WT (C) mice. The black arrows point to apoptotic figures, white arrow heads point to mitotic figures, filled black arrow heads point to Paneth cells and the open black arrow points to exfoliation. The B6 DKO ileum has enlarged crypts, lacks Paneth cells and have multiple apoptotic figures, while B6 TKO and WT ileum is unremarkable. Panel D. A box-and-whisker plot of ileal pathology score showing the median and interquantile range. The scores were determined from 21 male DKO, 22 male TKO, 13 female DKO, 12 female het-TKO (GPx1/2-DKO Nox1+/−), 4 WT and 7 Nox1-KO mice. The groups with different letters have different medians, where a>b>c. When the groups share the same letter are not different; i.e. ab is is not different from a or b groups and bc is not different from b or c groups. Panel E. A bar graph of the mean number of apoptotic figures per crypt in mouse ileum. The number of mice in each group is 18 male DKO, 16 male TKO, 9 female DKO, 5 female het-TKO, 4 WT and 7 Nox1-KO mice. The groups with different letters have different mean, where a>b>c. Panel F. A bar graph of average number of mitotic figures per crypt in mouse ileum. The number of mice in each group is 17 male DKO, 17 male TKO, 10 female DKO, 4 female het-TKO, 4 WT and 7 Nox1-KO mice. The error bars in E and F are one SD.

NIH-PA Author Manuscript
NIH-PA Author Manuscript
NIH-PA Author Manuscript

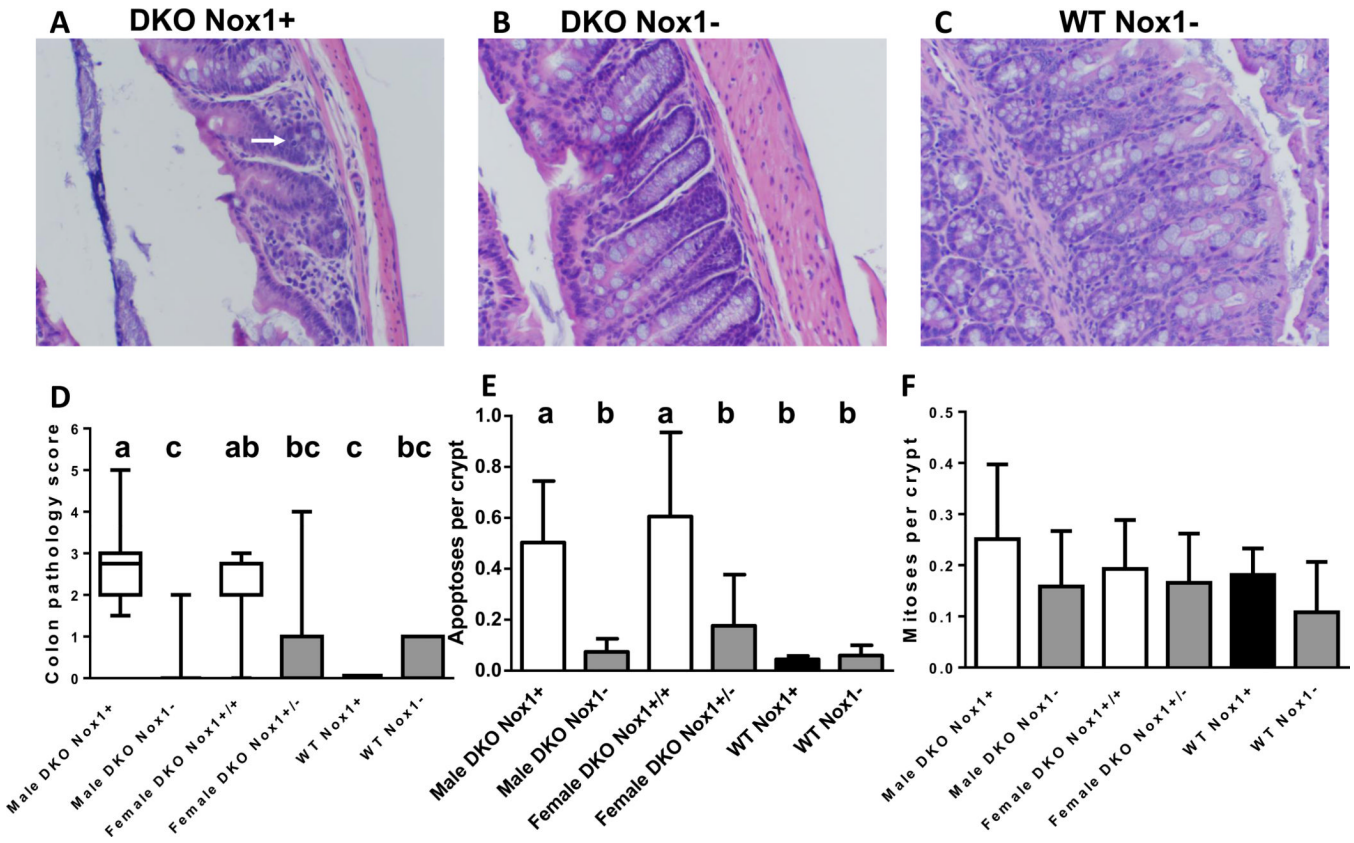

Figure 5.

Colon histology, pathology scores and number of apoptotic and mitotic figures per crypt in 50-day-old mice. Panels A-C are representative H&E-stained colon sections from a male DKO (A), TKO (B) and WT Nox- (C) mice. The white arrow points out a slightly distorted gland with mucin depletion. DKO mice had few goblet cells, which are present in TKO (DKO Nox1−) and abundant in the WT Nox1− mouse. Panel D. A box-and-whisker plot of colon pathology score showing the median and interquantile range. The scores were determined from 20 male DKO, 20 male TKO, 13 female DKO, 11 female het-TKO (DKO Nox1+/−), 4 WT and 7 Nox1-KO mice. Different letters above the boxes indicate different medians (Panel D), where a>b>c. Groups that share the same letter are not different; i.e. ab is not different from a, and bc is not different from c. Panel E. A column graph showing the mean of apoptotic figures per crypt in mouse colon. The number of mice in each group is 16 male DKO, 15 male TKO, 9 female DKO, 5 female het-TKO, 3 WT and 6 Nox1-KO. Groups with different letters are significantly different, where a>b. Panel F. A column graph of mean mitotic figures per crypt in mouse colon analyzed from the same number of mice in Panel E, except male DKO group has 17 mice. The error bars in E and F are one SD.

NIH-PA Author Manuscript
NIH-PA Author Manuscript
NIH-PA Author Manuscript

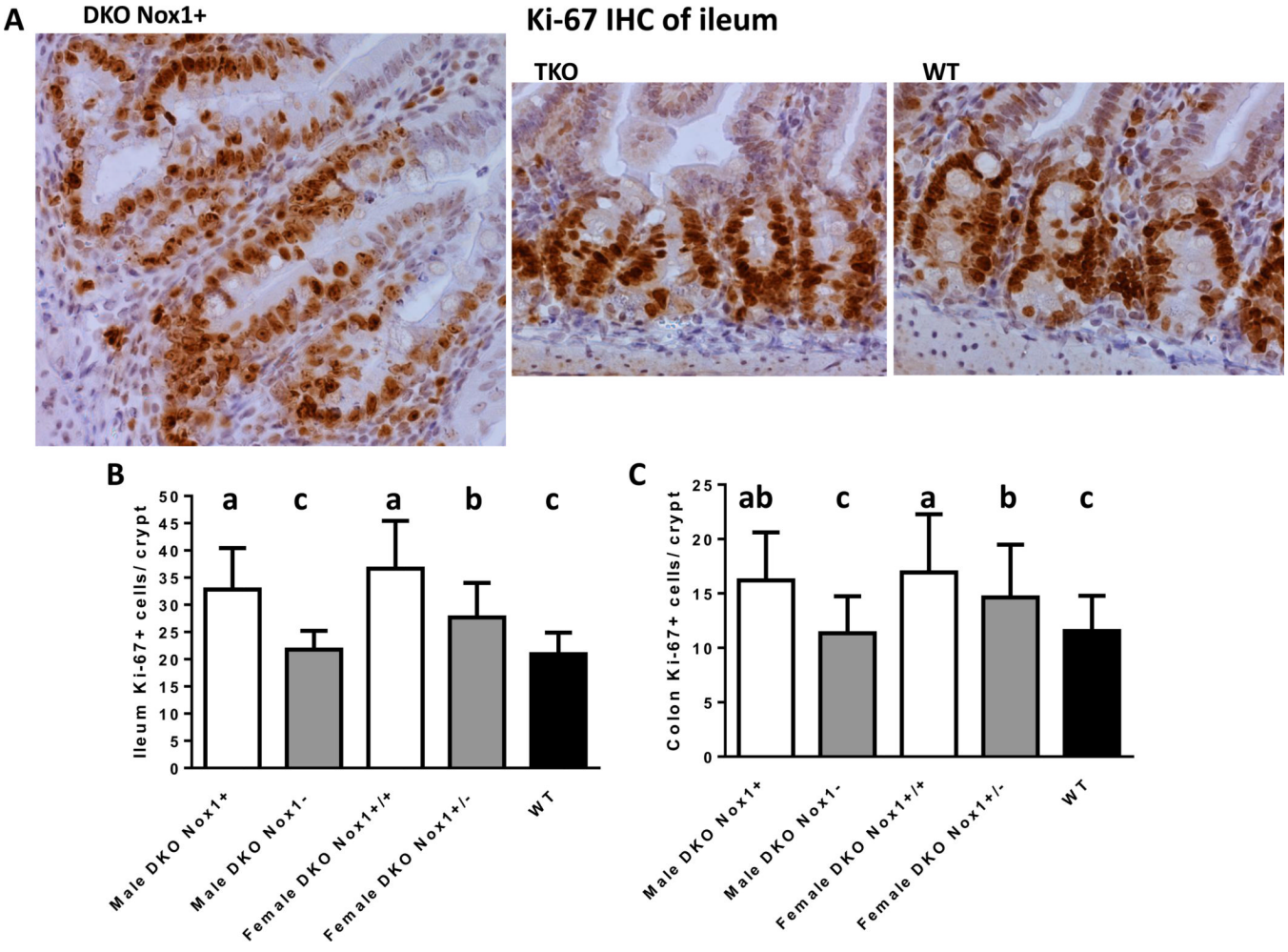

Figure 6.

IHC of Ki-67 in ileum and analysis of Ki-67 positive (+) cells in the crypt of ileum and colon. Panel A show representative crypts from a DKO (Nox1+), TKO and WT mice. Panels B and C are column graphs of mean number of crypt Ki-67+ cells in the crypt of ileum and colon. The number of mice in each group is 4 male DKO, 6 male TKO, 4 female DKO, 5 female het-TKO and 5 WT mice. Eight to 18 crypts were counted per mouse. Groups with different letters are significantly different, where a>b.c. When groups share the same letter are not different, i.e. ab is not different from a or b. Error bars are one SD.

NIH-PA Author Manuscript
NIH-PA Author Manuscript
NIH-PA Author Manuscript

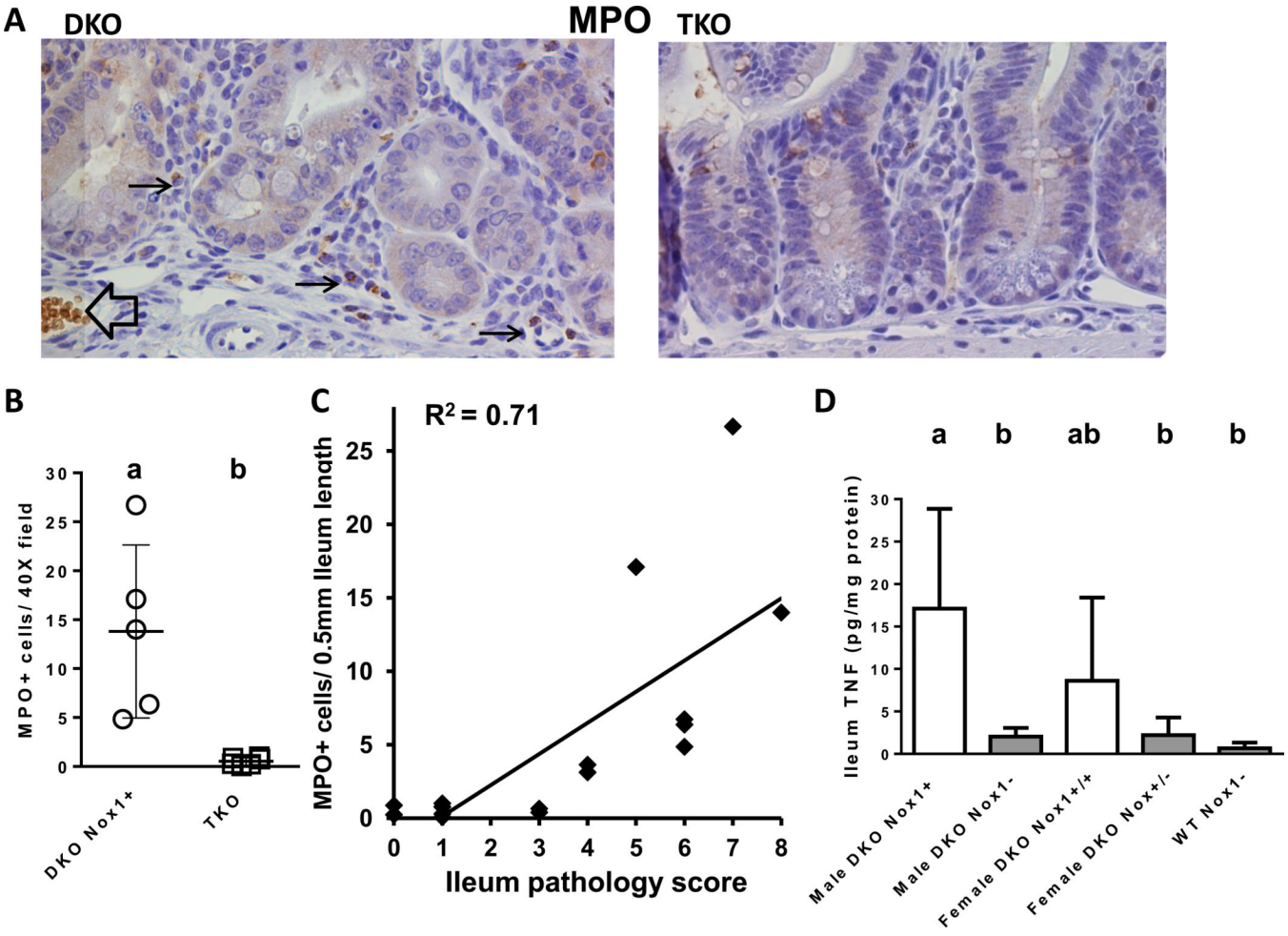

Figure 7.

Analysis of MPO-positive infiltrating cells and TNF levels in the ileums of DKO and TKO mice. Panel A. MPO IHC of DKO and TKO ileum. The black arrows point to the positive stained monocytes in the submucosa of the crypt. The black open arrow points to a blood vessel and spuriously stained red blood cells. Panel B. A scatter plot of MPO+ cells analyzed in 50-day-old 5 DKO and 6 TKO males. The DKO group has higher number of MPO+ cells than TKO group (i.e. a>b; P=0.0048). Panel C. Correlation of MPO+ cells with ileum pathology scores. The correlation was made from all 11 mice in Panel B and five 28-day-old DKO mice. There is a positive correlation between MPO+ cells and pathology score with R^2=0.71 (non-parametric). Panel D. A bar graph of TNF levels in mouse ileum at 50 days of age. The number of mice in each group is 3 male DKO, 8 male TKO, 4 female DKO, 6 female het-TKO and 8 WT Nox-mice of both genders. The error bars are SD. Groups with different letters are significantly different, where a>b. The groups share the same letter are not different, i.e. ab is not different from a or b.

NIH-PA Author Manuscript
NIH-PA Author Manuscript
NIH-PA Author Manuscript

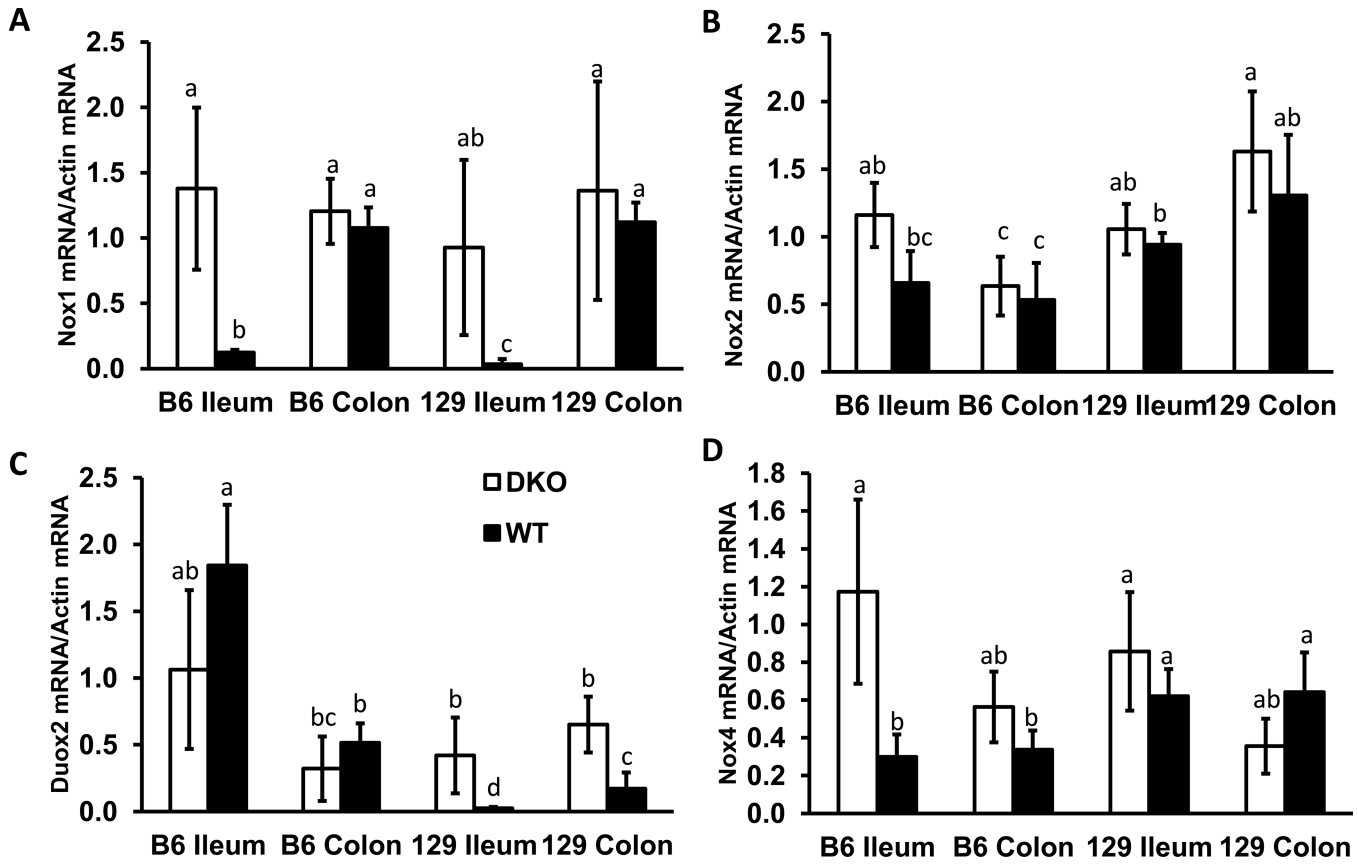

Figure 8.

Comparison of Nox1, Nox2, Duox2 and Nox4 mRNA levels in the ileum and colon of B6 and 129 DKO and WT mice at 30 days of age. The mRNA levels were normalized against β-actin. Each group has 4 mice, error bars are SD. Groups with different letters are significantly different, where a>b>c>d. The groups share the same letter are not significantly different, i.e. ab is not different from a or b, and bc is not different from b or c.

NIH-PA Author Manuscript

NIH-PA Author Manuscript

NIH-PA Author Manuscript

Table 1

Real-time PCR primer sequences for mouse cDNA

B-Actin	Forward 5'-GCTCCTCCTGAGCGCAAGT-3'
	Reverse 5'-TCATCGTACTCCTGCTTGCTGAT-3'
Duox2	Forward 5'-TCACAACGGACGGCTTGCCC-3'
	Reverse 5'-CCCGGCCACTCCATTGCTGG-3'
Nox1	Forward 5'-CTCCCTTTGCTTCCATCTTG-3'
	Reverse 5'- GCAAAGGCACCTGTCTCTCTA-3'
Nox2	Forward 5'-TGAGAGGTTGGTTCGGTTTT-3'
	Reverse 5'-GTTTTGAAAGGGTGGGTGAC-3'
Nox4	Forward 5'- ACAACCAAGGGCCAGAATACTACTAC-3'
	Reverse 5'- GGATGAGGCTGCAGTTGAGG-3'